Available online at www.sciencedirect.com
SCIENCE DIRECT
Thermochimica Acta 437 (2005) 17–20
thermochimica acta
www.elsevier.com/locate/tca

Thermodynamic properties for the system of silybin and poly(ethylene glycol) 6000

Wei-Wei Yao, Tong-Chun Bai *, Jian-Ping Sun, Cheng-Wen Zhu, Jie Hu, Hua-Li Zhang

Department of Chemistry and Chemical Engineering, Suzhou University, Suzhou 215006, China

Received 25 January 2005; received in revised form 6 June 2005; accepted 7 June 2005
Available online 14 July 2005

Abstract

Solid dispersions of silybin and poly(ethylene glycol) (PEG) 6000 were prepared by fusion-cooling. T–wt% and $\Delta_{fus}H_w$–wt% diagrams have been constructed by DSC method. A eutectic point with $wt_{sily}\% = 33.3$ and $T_{mE} = 324.3$ K was determined. IR spectroscopy and X-ray diffraction results indicates that the spectrum can be regarded as the superposition of those silybin and PEG 6000. There was no significant change in the crystal structure of silybin and PEG 6000 in their solid dispersion formulations. The experimental T–wt% and $\Delta_{fus}H_w$–wt% diagrams were fit with fair agreement by Flory–Huggins model.

Keywords: Silybin; Poly(ethylene glycol) 6000; Phase diagram; Enthalpy of fusion; Flory–Huggins model

1. Introduction

Drugs are mainly hydrophobic organic compounds. The solubility and dissolution rate of biologically active compounds are often limiting factors for their applicability. Therefore, the solubility/dissolution enhancement of drugs is an important task in pharmaceutical technology, because it leads to a better bioavailability. Among the techniques to increase drug dissolution rate, the formulation of solid dispersions is one of the most popular methods [1–3]. However, there are still some problems limiting the application of solid dispersions. For example, the preparation method by fusion at higher temperature usually causes drug decomposition. An optimum carrier not only spreads drug uniformly but also decreases the melting temperature of the formulation. Therefore, data on enthalpy of fusion and the phase diagram of solid–liquid equilibrium for solid dispersions are essential.

The molecular structure of silybin is shown in Fig. 1. Possibly due to its antioxidant and membrane stabilizing properties, the compound has been shown to protect different organs and cells against a number of insults. Its use has been widespread since preparations became officially available for clinical use. A major problem in the development of an oral solid dosage form of this drug is the extremely poor aqueous solubility, possibly resulting in dissolution-limited oral absorption [4].

Polymers, such as poly(ethylene glycol) (PEG) and poly(vinylpyrrolidone) (PVP), have frequently been used as carrier in solid dispersion formulations [2,3]. PEGs are widely used due to their low melting point, low toxicity, high viscosity, wide drug compatibility and hydrophilicity [2,5,6]. The molecular weight used in the formulation of solid dispersions ranges from 1000 to 20 000.

In this work, the thermodynamic properties of solid dispersions of silybin with PEG 6000 were determined. Our aim is to study the possible effect of PEG on decreasing the melting temperature of solid dispersions. The melting temperature, T_m, and the enthalpy of fusion, $\Delta_{fus}H$, were measured by differential scanning calorimetry (DSC). The phase diagram and the enthalpy diagram were constructed from experimental data. The data were fit to the Flory–Huggins model. FT-IR spectroscopy and powder X-ray diffraction were performed to elucidate the structure and possible drug–carrier interactions.

* Corresponding author. Tel.: +86 512 65112645; fax: +86 512 65224783.
E-mail address: tcbai@suda.edu.cn (T.-C. Bai).

0040-6031/$ – see front matter © 2005 Elsevier B.V. All rights reserved.
doi:10.1016/j.tca.2005.06.012

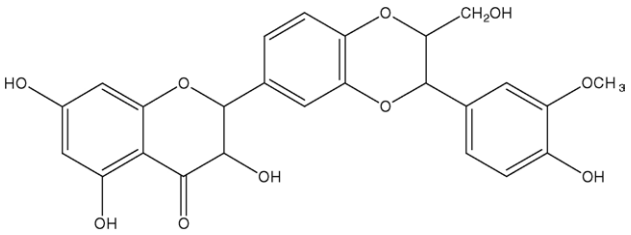

Fig. 1. Chemical structure of silybin.

2. Materials and methods

2.1. Materials

Silybin was purchased from Panjin Green Biological Development Co. Ltd., Liaoning, China. Its purity was claimed to be 97% by UV-spectrometry at 252–288 nm. This purity was confirmed by our HPLC measurement. Silybin, 96.8%; isosilybin, 1.1%; silydianin, 0.8%; silychristin, 0.1% and other impurities, 1.2%. Before experiment, the drug was dried under vacuum at 353 K over 24 h. Analytical grade poly(ethylene glycol) 6000 was received from Shanghai Chem-Reagent Co. Both reagents were stored over P_2O_5 in a desiccator before use.

2.2. Preparation of solid dispersions

Solid dispersions with different concentrations of silybin were prepared by heating accurately weighed amounts of PEG 6000 and silybin in a glass container in a water bath at 353 K. The mixtures were ground in an agate mortar for more than 1 h, and then rapidly cooled in liquid nitrogen (flash cooling) for more than 30 min. Subsequently, the solid was stored over P_2O_5 in a desiccator for more than 72 h until use.

Here, the system is treated as a pseudo binary mixture composed of silybin and PEG 6000. This approach simplified the difficulties arose from multi-component, and in some cases has excellent predicting ability [7].

2.3. Differential scanning calorimetry (DSC)

DSC measurements were carried out with a Perkin-Elmer DSC-7 differential scanning calorimeter (Perkin-Elmer, Norwalk, USA) with a liquid nitrogen subambient accessory. Certified indium wire encapsulated in an aluminum crucible (supplied by instrument manufacturer) was used for temperature and heat flow calibration. An aluminum pan and lid without pinhole were used to contain the sample. An empty container of the same type was employed as a reference. Nitrogen gas of 99% purity was used as purge gas for all the experiments performed at a rate of 20 ml/min. Samples (3–8 mg) were weighed to ±0.1 mg. Balance model: FA 1004, Shanghai balance instrument factory. A mass loss profile of pure silybin solid was measured by TG. PE-DELTA SERIES 7, with N_2 flow rate: 20 ml/min. The TG curve shows that silybin is decomposed above 473 K. In DSC measurements, samples were heated at a scanning rate of 5 K/min, over a temperature range from 303 to 473 K. Peak temperature, onset temperature and enthalpy of fusion were determined for all samples (using the software attached to DSC apparatus). All materials and solid dispersions were performed in triplicate.

2.4. Infrared spectroscopy

Fourier transform-infrared (FT-IR) spectra were obtained on a Magna 550 FT-IR system (Nicolet, USA) with the KBr disk method. The scanning range was 400–4000 cm^{-1} and the resolution was 2 cm^{-1}.

2.5. X-ray powder diffraction

Powder X-ray diffraction investigations were performed with a Rigaku D/max-3C diffractometer (Japan), Cu Kα, voltage: 40 kV, and 35 mA, with the angular range of $10^\circ < 2\theta < 40^\circ$ in a step scan mode (step width 0.02).

3. Results and discussion

3.1. Silybin–PEG 6000 phase diagram

DSC tracings for silybin, PEG 6000 and some of the solid dispersions are shown in Fig. 2. The melting temperature is evaluated at the peak onset. The profile of silybin (Fig. 2, curve J) shows a single endothermic peak at the melting temperature 423.5 K with enthalpy of fusion 93 $J\,g^{-1}$. Sample of PEG 6000 (Fig. 2, curve A) displays a melting endotherm with a shoulder at the lower side, which indicates the presence of more than one crystal form of PEG. The lower transition corresponds to the defolding of a once folded form [2,8]. The temperature of onset point corresponding to the main peak of PEG 6000 is 333.9 K with an enthalpy of fusion 209 $J\,g^{-1}$.

For samples of solid dispersion with the composition lower than 33.3% (w/w) of silybin, the DSC profiles (Fig. 2, curves B–E) showed the absence of silybin peaks. This result suggests that silybin was completely soluble in the liquid phase up to a concentration of 33.3%. Because the melting temperatures of eutectic composition (Fig. 2 curve E) and PEG are close, DSC profiles are the combination of two melting processes. With increasing silybin, the second endothermic peak corresponding to the drug started to appear and gradually shifted towards the melting of pure silybin (Fig. 2 curves G and I), but the second peak was very broad.

Phase diagram of silybin and PEG 6000 is represented in Fig. 3. The phase diagram can be considered as a special type of a eutectic in which the liquidus curve and the solidus curve are superimposed (curve CD). Similar phase diagrams have been observed in other PEG 6000 and drug systems [2]. Characteristics of eutectic point were evaluated with $wt_E\% = 33.3$ of silybin, $T_{mE} = 324.3$ K and $\Delta_{fus}H_{wE} = 97$ $J\,g^{-1}$.

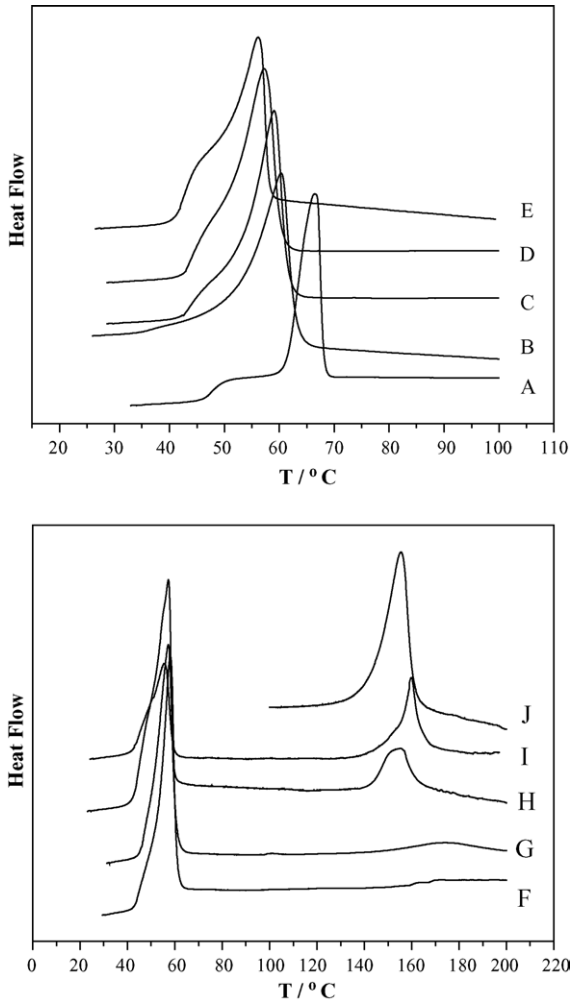

Fig. 2. DSC curves for solid dispersions of PEG 6000 and silybin. Mass percent of silybin: (A) 0; (B) 16.7; (C) 22.2; (D) 25.0; (E) 33.3; (F) 35.70; (G) 40.0; (H) 50.0; (I) 66.7; (J) 100.

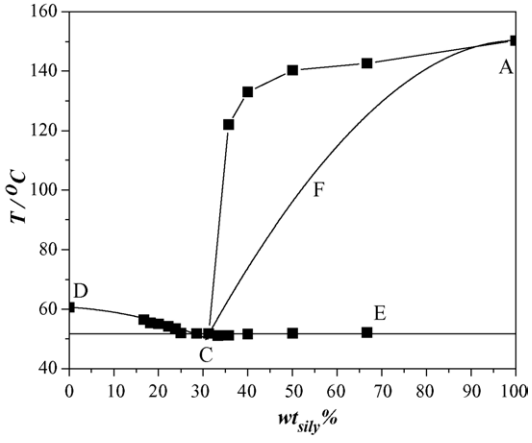

Fig. 3. Phase diagram for solid dispersions of silybin and PEG 6000: (■) experimental; line DC and AFC (—) Flory–Huggins model.

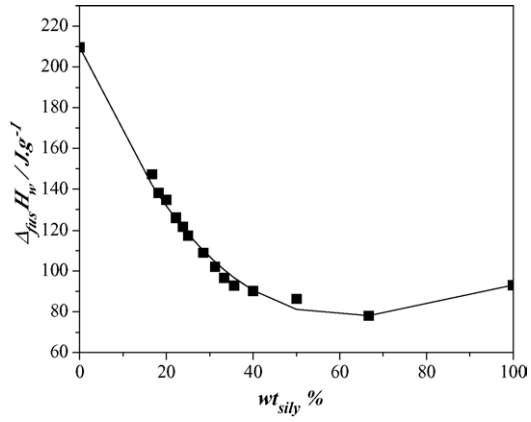

Fig. 4. The diagram of enthalpy of fusion for solid dispersion of PEG 6000 and silybin: (■) experimental; line (—) Flory–Huggins model.

3.2. Enthalpy of fusion

Fig. 4 shows the total melting enthalpy of two peaks for silybin and PEG 6000 mixture. The values of $\Delta_{fus}H_w$ decrease with the increase in weight percent, wt_{sily}%, of silybin.

3.3. FT-IR spectroscopy

To further study the possibility of an interaction of silybin with PEG 6000 in the solid state, more information was gathered using FT-IR spectroscopy. The possible interaction could occur between the –OH and –O– groups of PEG 6000 and –OH, –O– and C=O groups of silybin. Any interaction would be reflected by shifts in –OH, –O– and C=O vibration. The infrared spectra of silybin, PEG 6000 and some of their solid dispersions are shown in Fig. 5. Comparing the spectra of solid dispersions of silybin and PEG 6000 prepared by fusion-cooling (Fig. 5C and D assigned for wt_{sily}% = 50 and

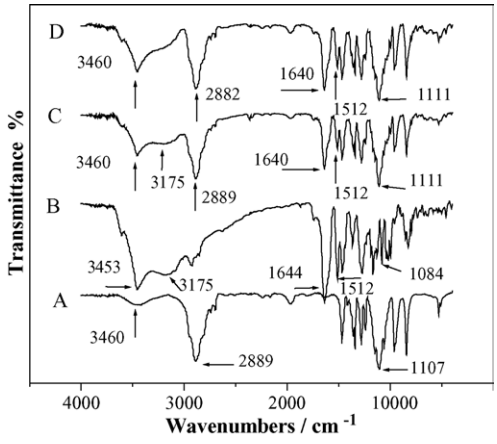

Fig. 5. FT-IR spectroscopy for solid dispersion of PEG 6000 and silybin. Mass percent of silybin: (A) 0; (B) 100; (C) 50; (D) 33.3.

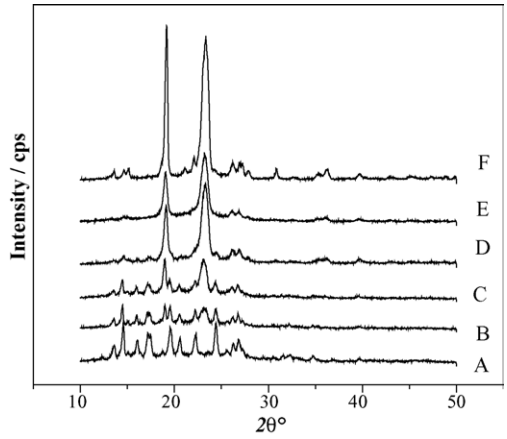

Fig. 6. X-ray diffraction patterns for solid dispersions of PEG 6000 and silybin. Mass percent of silybin: (A) 100; (B) 66.7; (C) 50.0; (D) 25; (E) 16.7; (F) 0.

33.3, respectively), no difference was observed in the position of the absorption bands. The spectra can be simply regarded as the superposition of those of silybin and PEG 6000. In Fig. 5B–D, the absorption band, assigned to the free OH, 3460 cm^{-1} is still present. However, the band assigned to OH due to intermolecular association at 3175 cm^{-1} is decreased in intensity in spectra C and D. Silybin hydrogen bonds to itself. When silybin is dispersed into PEG, this hydrogen bonding is decreased. No indication for hydrogen bonding between silybin and PEG was observed.

3.4. X-ray powder diffraction

Fig. 6 shows some of the X-ray diffractograms for silybin and PEG 6000 solid dispersions. The diffraction spectrum of pure silybin showed that the drug was crystalline as demonstrated by numerous distinct peaks. The characteristic peaks for PEG 6000 showed two peaks with highest intensity at 2θ of 19.16° (4.629 Å, *d*-spacing) and 23.32° (3.811 Å). Characteristic peak positions of silybin at 14.56° (6.079 Å), 17.20° (5.151 Å), 19.56 ° (4.535 Å) and 24.40° (3.645 Å) could also be detected in the samples with the carrier/drug weight ratio of 2:1 and 1:1. The peak at 19.56° (4.535 Å) in the samples prepared with the ratio of 3:1 and 5:1 (PEG 6000/silybin) could not be detected. These changes in the intensity of silybin might be explained as the result of the changes in crystal orientation.

From these observations we could deduce that the crystalline nature of silybin was still maintained, but the relative reduction of diffraction intensity of silybin peaks in PEG 6000 preparation at these angles suggested that the amount of drug in the samples is decreased and/or the quality of the crystals worsened. The positions of PEG 6000 patterns were the same in the solid dispersions, which ruled out the possibility of compound formation between PEG 6000 and silybin.

3.5. Fitting T_m and $\Delta_{fus}H$ by Flory–Huggins model

The Flory–Huggins model [9] was used to fit the melting temperature, T_m, and the enthalpy of fusion, $\Delta_{fus}H$. The liquidus curve of phase diagram was divided into two parts, the PEG and silybin rich regions, respectively. Corresponding to these two regions, the Flory–Huggins model is reformed to Eqs. (1) and (2), respectively:

$$\{\Delta_{fus}H^{\circ}_{m2}(T/T_{m2}) - RT[\ln\phi_2 + (1-\phi_2)(1-V_{m2}/V_{m1})]\} - \Delta_{fus}H^{\circ}_{m2} = \Delta w(1-\phi_2)^2 \quad (1)$$

$$\{\Delta_{fus}H^{\circ}_{m1}(T/T_{m1}) - RT[\ln(1-\phi_2) + \phi_2(1-V_{m1}/V_{m2})]\} - \Delta_{fus}H^{\circ}_{m1} = \Delta w\phi_2^2 \quad (2)$$

where subscript 1 and 2 are for silybin and PEG indices, $\Delta_{fus}H^{\circ}_{m}$ is the molar enthalpy of fusion, V_{mi} the molar volume of component, and ϕ is the volume fraction. In PEG rich region, the fitting result is shown in Fig. 3 curve DC with the model parameter $\Delta w = -369\,kJ\,mol^{-1}$. But in silybin rich region, experimental data is not sufficient to be fitted with an acceptable precision. Therefore, another approach was considered. At eutectic point, the value of T in Eqs. (1) and (2) are equivalent. Combining Eqs. (1) and (2), Δw was calculated to be $-17.3\,kJ\,mol^{-1}$. By this value, the predicted liquidus curve in silybin rich side is presented in Fig. 3 curve AFC. The predicted eutectic point is the cross point of lines DC and AFC ($wt_{E,sily}\%$ = 30.7 and T_{mE} = K). In order to fit the enthalpy of fusion, the model parameter, Δw, was assumed to be concentration dependent:

$$\Delta w = V_m[A + B(\phi_2 - \phi_1)] \quad (3)$$

where fitting parameter A is $-0.533\,kJ\,cm^{-3}$, and B is $-0.254\,kJ\,cm^{-3}$. V_m is the mole volume of the mixture. Fitting result is shown in Fig. 4 with fair agreement with experiment. The enthalpy of fusion at eutectic composition, $\Delta_{fus}H_{wE}$, was predicted to be $100\,J\,g^{-1}$.

References

[1] Abu T.M. Serajuddin, J. Pharm. Sci. 88 (1999) 1058–1066.
[2] F. Damian, N. Blaton, L. Naesens, J. Balzarini, R. Kinget, P. Augustijns, G. Van den Mooter, Eur. J. Pharm. Sci. 10 (2000) 311–322.
[3] G. Van den Mooter, P. Augustijins, N. Blaton, R. Kinget, Int. J. Pharm. 164 (1998) 67–80.
[4] F.-Q. Li, J.-H. Hu, Y.-Y. Jiang, J. Chin. Pharm. Sci. 12 (2) (2003) 76–81.
[5] S. Verheyen, P. Augustijns, R. Kinget, G. Van den Mooter, Thermochim. Acta 380 (2001) 153–164.
[6] F. Lacoulonche, A. Chauvet, J. Masse, Int. J. Pharm. 153 (1997) 167–179.
[7] T.C. Bai, J. Yao, S.J. Han, J. Chem. Eng. Data 44 (1999) 491–496.
[8] Z. Naima, T. Siro, G.-D. Juan-Manuel, C. Chantal, C. Rene, D. Jerome, Eur. J. Pharm. Sci. 12 (2001) 395–404.
[9] W.E. Acree Jr., Thermodynamic Properties of Nonelectrolyte Solutions, Academic Press Inc., Orlando, 1984.